Methodological developments for improved bottom detection with the ME70 multibeam echosounder

Sébastien Bourguignon[1, *], Laurent Berger[1], Carla Scalabrin[1], Ronan Fablet[2] and Valérie Mazauric[3]

[1] Ifremer, Centre de Brest, Z.I. Pointe du Diable, BP 70, 29280 Plouzané, France
[2] Telecom Bretagne, Technopôle Brest-Iroise, CS 83818, 29238 Brest Cedex 3, France
[3] Ifremer, Siège Social, Technopolis 40, 155 rue Jean-Jacques Rousseau, 92138 Issy-les-Moulineaux, France

*: Corresponding author : S. Bourguignon, tel: +33 492 003 029; fax: +33 492 003 121; email address : sebastien.bourguignon@oca.eu

Abstract:

Multibeam echosounders and sonars are increasingly used in fisheries acoustics for abundance estimation. Because of reduced side-lobe levels in the beam-array pattern, the new Simrad ME70 multibeam echosounder installed on board Ifremer's RV "Thalassa" has been designed to allow improved detection of fish close to the seabed. To achieve this objective, precise and unambiguous detection of the water-bottom interface is required, which raises the issue of bottom detection, especially in the outer beams. The bottom-detection method implemented in the ME70 is based on the amplitude of the reverberated echo. Such an approach is efficient for vertical beams, but less accurate for beams with higher incidence angles, typically 30°–40° for the beam configurations used on RV "Thalassa", where the incidence angle, the beam opening, and the nature of the seabed contribute to weakening the backscattered signal. Therefore, the aim of this study was twofold. First, we proposed to improve the current bottom-detection method based on the amplitude of the echo. Thanks to the split-beam configuration being available for all beams of the ME70, we also proposed to use the phase information in the backscattered signals of the outer beams, as is more commonly done with multibeam systems dedicated to seabed mapping. Then, we set a Bayesian estimation framework that takes into account the spatial continuity between adjacent echoes, giving more robustness to the bottom estimation itself. Results using data collected at sea for various bottom types are presented here.

Keywords: acoustics, bottom detection, fisheries, multibeam echosounder

1

Introduction

Acoustic methods are widely used in fishery research (Simmonds and MacLennan, 2005). In particular, echo-integration has become a standard technique for estimating fish abundance. Underwater acoustics is also a key tool for studying fish behaviour (Misund, 1997). In such applications, correct location of the water-bottom interface is crucial, because it sets the lower limit of the water column that can be used for fish detection and possibly biomass estimation.

A new, multibeam echosounder (ME70) was recently developed by Simrad in collaboration with Ifremer, opening new perspectives for fishery research (Trenkel et al., 2008). Traditional single-beam echosounders can sample the water column, with no interference from the bottom reverberation, inside a spherical volume whose radius is the bottom depth. Because of its higher side-lobe attenuation compared with conventional echosounders (up to −70 dB), the ME70 can collect data from outside this spherical volume in the outer beams, with the aim of detecting and studying demersal or semi-demersal fish: at 100-m depth and with a beam incidence of 35°, an 18-m high zone is defined above the seabed where fish detection is possible, despite contamination by the side lobes. Correct bottom detection is then a necessary preliminary step in defining precisely the beginning of the dead zone in the outer beams. The dead zone is the portion of the echo that is obscured by the bottom reverberation in the main lobe of the beam. See Ona and Mitson (1996) for a detailed description of the acoustic dead zone near the seabed.

The bottom-detection algorithms implemented in most fishery echosounders are amplitude detectors. Because the highest reverberation level is usually that caused by the seabed, the bottom is detected at the depth where the amplitude of the reverberated echo exceeds some given threshold. The user can then define the useful part of the water-column echo for biomass integration, which may include a backstep distance to ensure that no contribution from the bottom is included within the echo integral. If such a method performs well with vertical echosounders and reasonably flat seabeds, it may lead to unsatisfactory detection when the incidence angle increases, because the leading edge of the echo amplitude is not steep enough to provide a precise detection of the seabed. Such a problem arises for bottom detection in the outer beams of the ME70 (Trenkel et al., 2008). Bottom detection based on amplitude thresholding suffers from a similar problem when a beam with normal incidence hits a sloping seabed. The sharpness of the leading edge can also be affected by the seabed type and reflection properties (Pouliquen and Lurton, 1994; MacLennan et al., 2004). The presence of dense fish schools close to the seabed may also cause false detections, because the

bottom may be erroneously detected as being above the school. This effect requires supervision by the user to manually perform some post-processing to draw a new bottom line that includes the corresponding biomass (Foote *et al.*, 1991; Ona and Mitson, 1996). Thus, the design of a robust procedure to automatically correct false bottom detections is a challenge aimed at reducing the number of burdensome bottom corrections that have to be made manually.

Two issues aimed at improving bottom detection were studied and are presented in this paper. The first deals with the extraction of relevant information from the backscattered signal for all beams of the ME70. Specifically, because all beams of the ME70 can be configured in split-beam mode, phase differences in both along-ship and athwartship directions are available (Carlson and Jackson, 1980). Using phase information instead of or together with amplitude data may provide more accurate results for bottom detection in the outer beams, as performed in bathymetry (Lurton, 2002). In addition, MacLennan *et al.* (2004) revealed the potential of phase-difference data to discriminate between fish and seabed echoes. Second, a robust statistical framework is proposed to take account of the spatial continuity of the seabed in both alongship and athwartship directions for multibeam data. The objective is to bring greater stability to the whole detection process, specifically by correcting erroneous bottom detections.

In this paper, typical amplitude and phase signals are described and preprocessing steps to obtain one or several possible locations of the water-bottom interface from single-beam data are detailed. Then, a simple model is described that takes account of the spatial continuity of the detected bottom between consecutive pings or between adjacent beams of the ME70. An easily implemented filtering algorithm is proposed, which merges both information sources, single-beam detection and bottom continuity, to provide a real-time estimation of the seabed location. Applications to experimental data are reported, displaying satisfactory results in both the vertical and the outer beams.

Backscattered-signal analysis and single-beam bottom detection

This section focuses on the shape of the amplitude and phase shifts of the backscattered signal. The aim is to extract likely locations for the water-bottom interface. For both signals, some preprocessing steps are proposed to account for noise and signal variability.

Amplitude-based detection

Because the reflection coefficient of the seabed is usually much higher than that of fish schools, bottom detection based on the echo amplitude is a natural choice, as implemented in current fishery echosounders. The shape of the leading edge, however, depends on many parameters, including the nature of the seabed, the depth, the beam width, and, most importantly, the angle between the incident beam and the seabed (Lurton, 2002).

Amplitude thresholding: efficiency and limits

Figure 1 shows the amplitudes of typical backscattered signals acquired by Simrad ER60 and ME70 echosounders at normal incidence and by the ME70 echosounder at incidence 33°. These data were acquired at locations very close to each other, and thus are characterized by the same depth and bottom type. Amplitude-based detection is usually performed by thresholding the signal at some level before it peaks. Then, a backstep distance
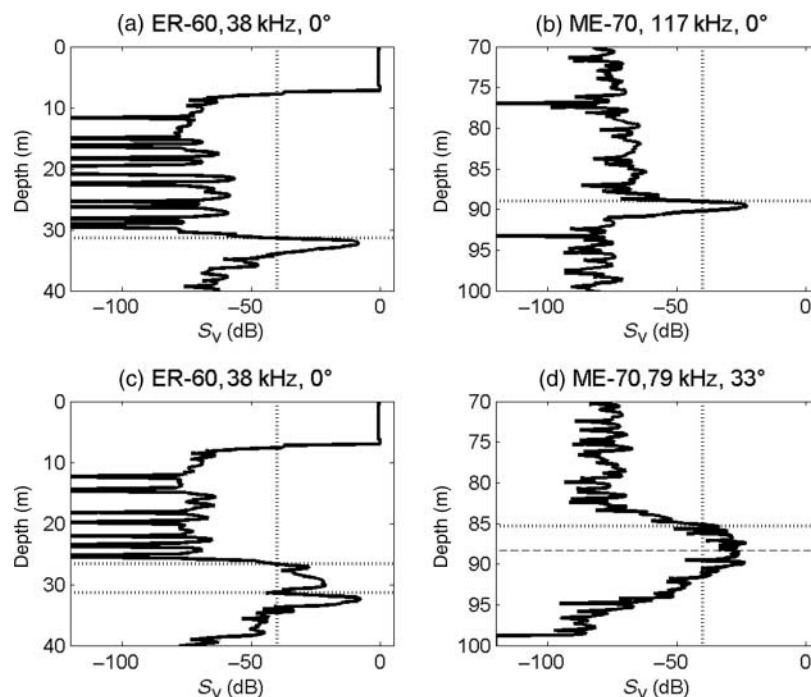

Figure 1. Examples of backscattered signals where the echo amplitude is expressed as volume-backscattering strength (S_v in dB). ER60 normal incidence-angle data, 38 kHz, S_v values for two pings: without fish (a) and with fish near the seabed (c). ME70 data, vertical beam (b), and outer beam with incidence angle of 33° (d). Amplitude data (full line), bottom detection (horizontal dotted line) based on a threshold of −40 dB (vertical dotted line). The full line in (d) locates the estimated bottom by maximum-amplitude detection for non-normal incidence angles.

is applied to ensure that no contribution from the bottom is included within the echo integral of the water column (Ona and Mitson, 1996). To reduce interference from noise, a smoother amplitude signal should be considered, especially for non-normal incidence angles. Here the amplitude data are low-pass filtered by a Hanning filter with a cut-off frequency at 0.8 m^{-1}. This gives a smooth, but still useful signal for any echosounder and any incidence angle, as illustrated in Figure 1. Figure 1a and b illustrates situations where a threshold-based detection method works perfectly at normal incidence angles. In Figure 1c, however, the bottom-detection threshold is crossed at a lower depth, because there are fish close to the seabed. In such a case, manual correction by the user is required to accurately locate the bottom and to integrate the corresponding biomass. In Figure 1d (non-normal incidence angle), thresholding at -40 dB locates a point in the middle of the leading edge, which is much wider than at normal incidence angles, and does not give a satisfactory detection.

Non-normal incidence angles: maximum-amplitude method

At non-normal incidence angles, locating the bottom and defining the useful portion of the echo for fish detection are two different issues. Once the bottom has been detected, it is necessary to use a wider backstep zone with some "adaptive" width, because the shape of the leading edge itself depends on the beam width and incidence angle, and it shows high variability from one ping to another. In practice, the use of multibeam data emanating from close to the seabed first requires locating the bottom. Second, the upper limit of the backstep to avoid any seabed contribution should be determined. In this paper, only the bottom-detection problem is considered.

Following methods used for bottom detection at small incidence angles for bathymetric applications (Lurton, 2001), we computed the bottom position from the filtered amplitude signal as the barycentre (in terms of energy) of that portion of the signal where the amplitude was >10 dB less than the maximum. The reason for this approach was to gain robustness in noisy conditions.

Non-normal incidence angles: phase-difference cancellation method

All the ME70 echosounder beams can be configured in the split-beam mode. The split-beam configuration is mainly used to compensate for transducer directivity in target-strength measurements (Ehrenberg, 1983). However, phase information from split-beam measurements can also be used to detect the water-bottom interface, for example, for seabed mapping, where, as the incidence

angle increases, bottom detection switches from amplitude-based to phase-based methods. The main beam is split into two parallel and closely spaced secondary beams. Then, the phase difference between these secondary beams is zero when the centre of the beam arrives at the bottom (Lurton, 2001). The goal then is to detect zero-crossings in the phase signal.

Typical phase data for several incidence angles are displayed in Figure 2. To gain robustness in the presence of noise, some preprocessing is necessary to efficiently use the phase information. In practice, the phase signal is first passed through a five-element mean filter. Then, the zero crossing closest to the amplitude maximum is located. For negative incidence angles, the sign of the athwartship angle should change from positive to negative, and conversely for positive incidences. As illustrated in Figure 2, it is difficult to detect the phase cancellation for low incidence angles. Conversely, at greater incidence angles, the phase reveals an almost linear shape around the location of the bottom depth. In such a case, a zero crossing can be detected.

Practical considerations

Many tests were conducted to compare the maximum-amplitude and phase-difference-cancellation methods for bottom detection using the ME70. The methods were applied to different datasets obtained with different configurations of the ME70, varying depths, and seabed types, while the seabed was approximately flat. Figure 3a illustrates typical standard deviations of the estimated bottom position as a function of the incidence angle. Below 20°, the maximum-amplitude method exhibits less variability. Conversely, for incidences $>20°$, the phase-cancellation method is more robust. Typical bottom lines illustrating this behaviour are depicted in Figure 3b. In practice, the maximum-amplitude and phase-cancellation methods should be used, respectively, for incidence angles less than and greater than 20°.

A state–space framework for robust bottom detection

Here we deal with a Bayesian estimation framework for bottom detection. It relies on the definition of a likelihood function that describes the confidence in amplitude- or phase-based bottom detection. Further, a state–space, prior model is proposed to take account of the regularity of the bottom between two consecutive pings. Using Bayesian particle filtering, both information sources are merged and a robust estimate of the bottom location is computed.
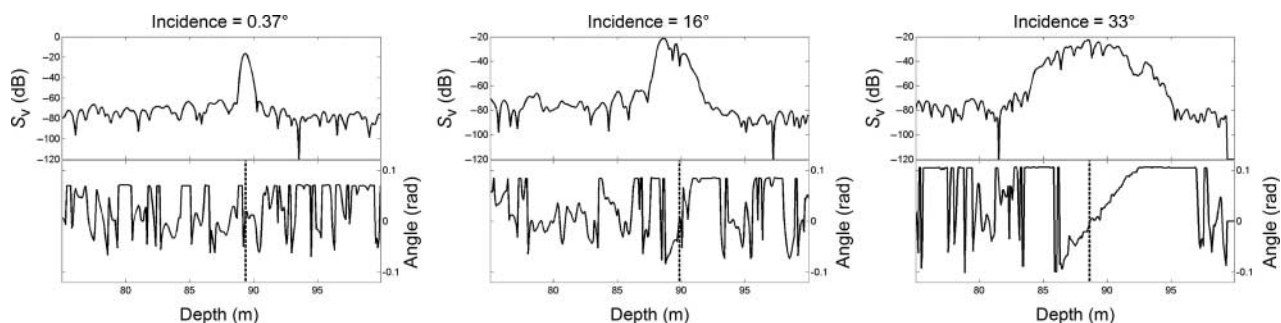

Figure 2. Echo amplitudes (top) and athwartship phases (bottom) for incidence angles of 0.37° (left), 16° (centre), and 33° (right), obtained from ME70 split-beam data. The expected depth is ∼90 m. The full lines plot the raw angle data and the vertical dashed lines locate the detection of phase cancellation.

Statistical description of bottom detection

For the sake of clarity, only single-beam data are considered here. Suppose that for ping k, the true bottom location is at depth z_k and has been detected at depth y_k, by amplitude-maximum, phase-cancellation, or any other method. Then $y_k = z_k + e_k$, where the error e_k is unknown. Suppose that $\{e_k\}_k$ is a sequence of independent random variables, according to some probability distribution: $e_k \sim p_k(e_k)$. Then, the likelihood function (Edwards, 1972) is defined as $L(y_k|z_k) \propto p_k(y_k - z_k)$. With no additional knowledge of the error statistics, the Gaussian assumption is the most reasonable choice

$$p_k(e_k) = g_\sigma(e_k) \equiv \frac{1}{\sigma\sqrt{2\pi}} \exp\left(-\frac{e_k^2}{2\sigma^2}\right). \quad (1)$$

That is, the most likely value for z_k is y_k with some uncertainty expressed by the variance σ^2 (Figure 4a).

A more robust choice is to consider a mixture model composed of Gaussian and uniform distributions for $p(e_k)$. Then the most probable value is y_k, but errors occur elsewhere with a higher prob-
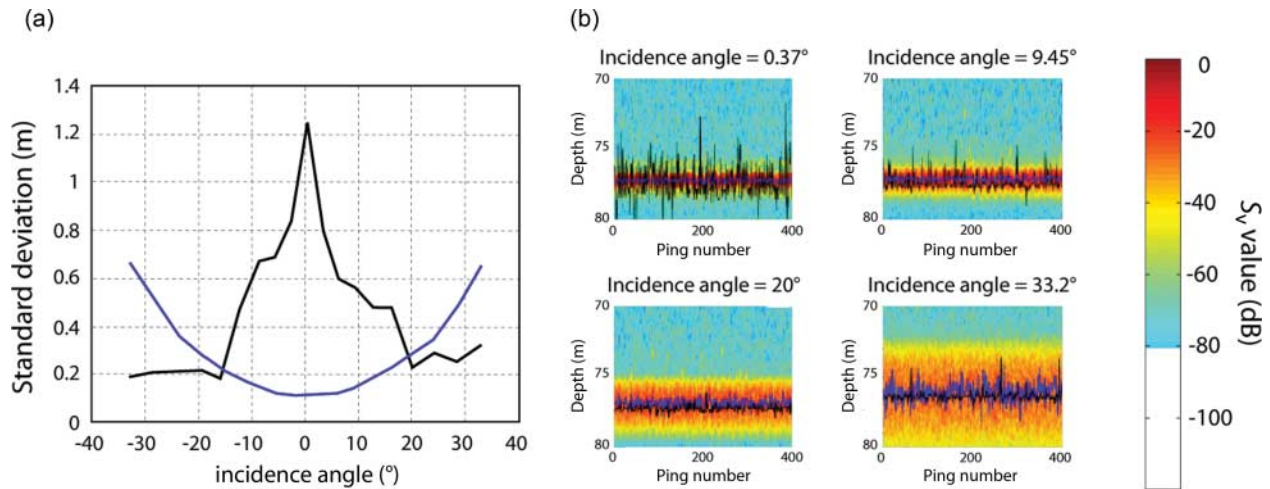

Figure 3. (a) Standard deviation of the bottom location as a function of the incidence angle and the method of detection: maximum-amplitude (blue line) and phase-cancellation (black line). (b) Typical bottom lines obtained by maximum-amplitude (blue) and phase-cancellation (black) at different incidences.
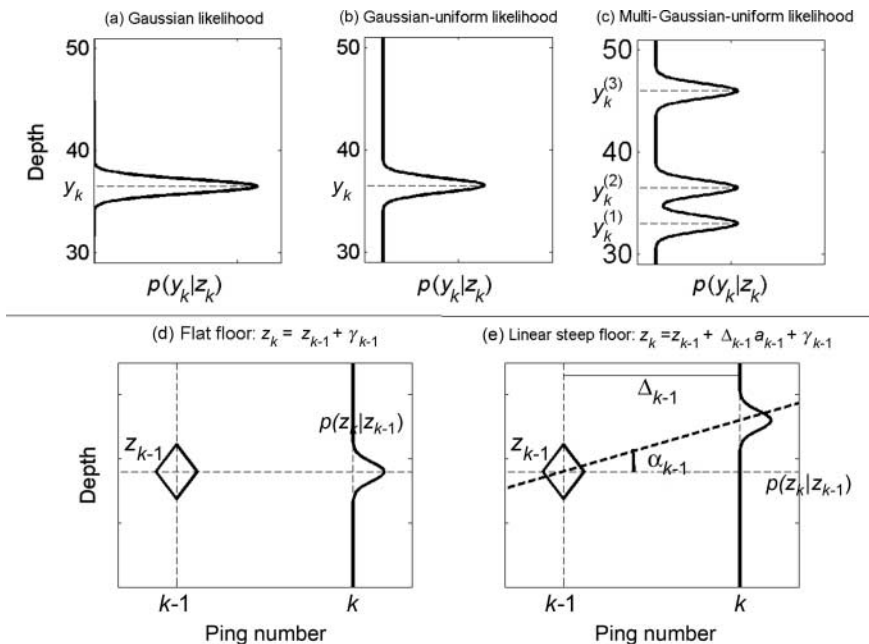

Figure 4. Gaussian, Gaussian-uniform, and multi-Gaussian-uniform likelihood functions (a, b, and c). prediction models for bottom regularity: flat seabed (d) and linear steep seabed (e).

ability than for the Gaussian assumption (Figure 4b). To include the possibility of several candidates, say $y_k^{(p)}$, $_{p=1\ldots P}$ for bottom location (as in Figure 1c), we finally build a multimodal likelihood function where each mode corresponds to a possible value. Formally, this is written as

$$L(y_k|z_k) \propto \alpha U_\Delta(Z_k) + (1-\alpha)\sum_{P=1}^{p} g_\sigma(z_k - y_k^{(p)}), \qquad (2)$$

where U_Δ is the uniform distribution on some reasonable boundary interval $\Delta = [z_{\min}, z_{\max}]$ and $\alpha \in [0,1]$ sets the proportion of the uniform distribution in the mixture (Figure 4c).

Spatial regularity

Using the above notations, we introduce spatial regularity in expressing that z_k, the true bottom location at ping k, should be close to that at ping $k-1$. A simple model is

$$z_k = z_{k-1} + \gamma_{k-1}, \qquad (3)$$

where γ_k is random. If the seabed is flat between the vessel positions at pings $k-1$ and k, the mean of γ_k is zero. A slightly more refined model takes a slope parameter into account, thus

$$z_k = z_{k-1} + d_{k-1}a_{k-1} + \gamma_{k-1}, \qquad (4)$$

where d_{k-1} is the (known) linear distance covered by the ship between the two pings and a_{k-1} the (unknown) projection of the slope of the seabed at ping $k-1$ in the direction of ping k. For this model, γ_{k-1} represents the error made by linearly interpolating the bottom location at ping k from the bottom depth and slope at ping $k-1$. Here again, the errors γ_k can be supposed random and distributed according to some given probability distribution. Both models are illustrated in Figure 4d and e.

In matrix form, we write the following linear model:

$$\begin{bmatrix} z_k \\ a_k \end{bmatrix} = \begin{bmatrix} 1 & d_{k-1} \\ 0 & 1 \end{bmatrix}\begin{bmatrix} z_{k-1} \\ a_{k-1} \end{bmatrix} + \begin{bmatrix} \gamma_{k-1}^{(z)} \\ \gamma_{k-1}^{(a)} \end{bmatrix} \Leftrightarrow \mathbf{x_k}$$
$$= \mathbf{F_k}\mathbf{x_{k-1}} + \boldsymbol{\gamma_{k-1}}, \qquad (5)$$

where the 2×2 matrix $\mathbf{F_k}$ is known, the vector $\mathbf{x_k}$ collects the unknown bottom depth z_k and the slope a_k at ping k, respectively, and γ_k represents the prediction errors in both z_k and a_k. Model (5) is a state–space prediction model (West and Harrison, 1997) that describes the spatial regularity of the seabed in the alongship direction. Here γ_k is considered Gaussian, with zero mean and covariance

$$\text{Cov}(\gamma k) \equiv \sum_\gamma \equiv \begin{bmatrix} \text{var}\gamma_{k-1}^{(z)} & 0 \\ 0 & \text{var}\gamma_{k-1}^{(z)} \end{bmatrix} = \begin{bmatrix} \sigma_z^2 & 0 \\ 0 & \sigma_a^2 \end{bmatrix},$$

with given variances σ_z^2 and σ_a^2.

Under this assumption, model (5) can be presented as a probabilistic prediction term.

$$p(\boldsymbol{x}_k|\boldsymbol{x}_{k-1}) = \frac{1}{2\pi|\sum_r|}\exp\left(-\frac{1}{2}(\boldsymbol{x}_k - \boldsymbol{F}_k\boldsymbol{x}_{k-1})'\sum_\gamma^{-1}(\boldsymbol{x}_k - \boldsymbol{F}_k\boldsymbol{x}_{k-1})\right). \qquad (6)$$

Note that for multibeam data, the regularity of the bottom in the athwartship direction can be similarly described. For a given ping, a state–space model can be derived, similar to model (5), where the bottom depth and the athwartship slope for a given beam are expressed as linear functions of the same parameters for the adjacent beam.

Particle-filtering algorithm

Until now, the statistical framework has been based on the definition of the likelihood function (2) for bottom detection in every beam and for every ping, and the use of the linear state–space model (5) for bottom continuity.

Bayesian estimation theory gives a natural framework to perform statistical inference sequentially (Doucet *et al.*, 2001). At a given instant k (after the kth ping), the posterior probability distribution $p(\mathbf{x_k}|y_1, \ldots, y_k)$ is that of the unknown parameters $\mathbf{x_k}$ (bottom depth and slope for ping k), according to models (2) and (5), once the data $y_1, \ldots, y_k$ have been acquired, that is, the bottom-detection values have been obtained for the first k pings. According to Bayes' rule, $p(\mathbf{x_k}|y_1, \ldots, y_k)$ can be written.

$$p(\mathbf{x_k}|y_1, \ldots, y_k) = K \cdot L(y_k|\mathbf{x_k})p(\mathbf{x_k}|y_1, \ldots, y_{k-1}) \qquad (7)$$

where K is a normalizing constant, $L(y_k|\mathbf{x_k})$ the likelihood function (2), and $p(\mathbf{x_k}|y_1, \ldots, y_{k-1})$ is

$$p(\mathbf{x_k}|y_1, \ldots, y_{k-1}) = \int p(\mathbf{x_k}|\mathbf{x_{k-1}})p(\mathbf{x_{k-1}}|y_1, \ldots, y_{k-1})\mathrm{d}\mathbf{x_{k-1}}. \qquad (8)$$

The first term in the integral is the prediction term (6) and the second term is exactly the posterior probability at ping $k-1$.

Equations (4) and (5) demonstrate how to compute the posterior distribution. At ping k, bottom-detection methods are applied and the likelihood (2) is built. Then, the spatial regularity of the seabed expressed by model (5) is taken into account by the prediction term $p(\mathbf{x_k}|\mathbf{x_{k-1}})$ to formulate Equation (8), which is used, jointly with the likelihood function, to obtain the posterior distribution (7).

It is generally impossible to compute Equations (7) and (8) from an explicit analytical expression, except in very specific cases, such as when models are linear and all probability distributions are Gaussian, which is not the case here. The use of particle filters (Doucet *et al.*, 2001) is a very common and efficient way to approximate such distributions. Here we use the Sampling Importance Resampling filter, as detailed in the tutorial paper by Arulampalam *et al.* (2002). In practice, using $T = 250$ particles ensured a good approximation at low computational cost. Once such an approximation of Equation (7) is available, an estimate of the bottom depth can be obtained by taking the parameters $\mathbf{x_k}$ that maximize the distribution (the maximum *a posteriori* estimate), or by computing the mean of $\mathbf{x_k}$ according to its

posterior distribution (the posterior mean estimate). The latter option is chosen here; this algorithm is from now on referred to as the bottom-continuity particle-filtering (BCPF) algorithm.

320   The BCPF algorithm requires several parameters to be tuned. In the likelihood function (2), σ is the standard deviation of the Gaussian part of the error around the detected bottom. It is related to the sampling interval along the depth axis, which depends on the ME70 configuration. In all our experiments, the

325   depth-sampling interval of the ME70 was ~10 cm; therefore, σ was set to 10 cm. The proportion of uniform distribution in the mixture model (2) was set to $\alpha = 0.2$, that is, the likelihood is 20% uniform and 80% multi-Gaussian. This choice allows robustness against errors while preserving the information content

330   brought by the Gaussian part. In the prediction model (5), σ_z is the standard deviation of the prediction error on the bottom location, and it was set analogously to $\sigma_z = \sigma = 0.1$ m, the sampling interval along the depth axis. In the notation of model (5), σ_a is the standard deviation of the prediction error in $a_k =$

335   $\tan (\alpha_k)$; see Figure 4. In practice, we set $\sigma_a = 0.05$, which corresponds approximately to an error of $3°$ in the slope prediction.

Applications

Different datasets were used to test and validate the approach presented here. The first comprises echosounder data contaminated

340   by false bottom detections, caused by fish close to the seabed. Then, two examples with ME70 data are presented. In the first of these, the leading edge of the echo-amplitude in the outer beams is less sharp because the water is rather deep (200 m). In the second example, the dataset comprises multibeam obser-

345   vations of large and dense fish schools close to the seabed.

ER60 data, normal incidence

The echogram in Figure 5a was obtained during the PELGAS'06 fisheries survey in the Bay of Biscay, with a Simrad ER60 echosounder operating at 38 kHz and a pulse duration of 1024 μs.

350   The bottom-detection method uses an amplitude threshold, set during the survey at -40 dB. Some spikes are visible in the bottom line, caused by the presence of fish close to the seabed. In this example, the same threshold (-40 dB) was used for the first step of the proposed new method. The computed bottom

355   line has been added in Figure 5b, illustrating that the spikes have been removed. Figure 5c and d illustrates by expanded echogram views how the new method works. Several possible candidates for bottom detection are illustrated in Figure 5c. The best location of the interface between the bottom and the fish school is provided

360   by running the spatial-continuity algorithm. In Figure 5d, the standard amplitude-thresholding method locates the bottom as being above the fish, and there is no other threshold crossing between the fish and the bottom. In this case, allowing for detection errors, and considering spatial continuity, also permits a

365   correct location of the bottom.

ME70 data

Bottom detection with multibeam data acquired by the ME70 is performed in the following way:

(i) for incidences below $20°$, locate the maximum echo

370   amplitude,

(ii) for incidences above $20°$, locate the cancellation of the athwartship phase-difference signal, then
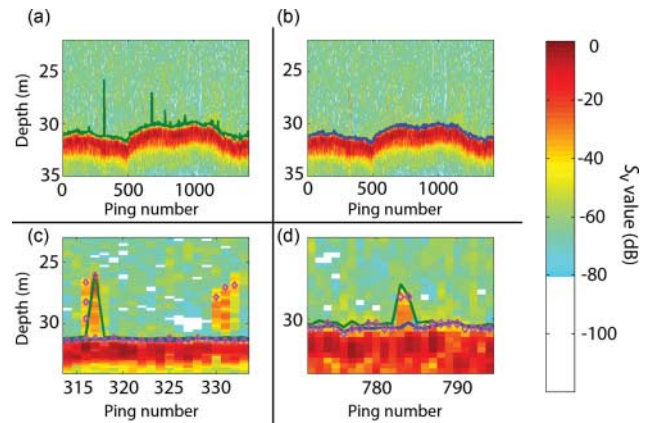

Figure 5. Bottom detection from ER60 echosounder data. (a) Bottom line computed by the standard firmware of the ER60. (b) Bottom line estimated using the BCPF algorithm. (c and d) Expanded views of two cases with false bottom detections. The magenta diamonds represent possible candidates for bottom detection, in this case, where the amplitude crosses a -40 dB threshold. The final result of the BCPF method allows an accurate estimation of the bottom (blue line) and an appropriate discrimination between fish and bottom echoes. Numerical values give, for each case, the mean bottom depth along the sequence and the corresponding standard deviation.

(iii) apply spatial-regularity criteria to the data for each beam using the BCPF algorithm.

Deep water (~200 m)

The data considered in this section were acquired during the EXACHA'08 technological survey in March 2008 in the Bay of Biscay. The ME70 was configured to have 21 beams incidence angles ranging from $-41°$ to $41°$ and 3-dB beam widths ranging   380 from $6°$ in the outer beams to $3°$ in the vertical beam. The pulse duration was 1024 μs and all beams were configured in split-beam mode. Echograms obtained at several incidence angles are displayed in Figure 6, where the vertical axis depicts the depth h and not the range d of the echo, thus $h = d \cos(\theta)$, where θ is   385 the incidence angle. Bottom detection by the ME70, mainly done with amplitude thresholding set at -40 dB, is not satisfactory in the outer beams, because the bottom is detected well above the location indicated by the echo maximum. Bottom detection based on maximum amplitude and phase cancellation   390 achieves more accurate results, but there are still spikes, especially at the highest incidences. The BCPF algorithm efficiently removes spikes and yields a more regular bottom line. Numerical estimates of the mean depth and the associated standard deviations in each case are given in Figure 6 and confirm   395 these findings, revealing yet more improvement as the incidence angle increases.

Shallow water, fish close to the seabed

Echograms in Figure 7 are from the IBTS'08 fisheries survey, carried out in the North Sea in January 2008. They display   400 dense herring schools located close to the seabed. The ME70 was configured to have 15 beams in split-beam mode, with incidence angle ranging from $-50°$ to $50°$ and 3-dB beam widths ranging from $10°$ in the outer beams to $5°$ in the vertical beam. The pulse duration was 1024 μs. Because of the strong backscattering   405
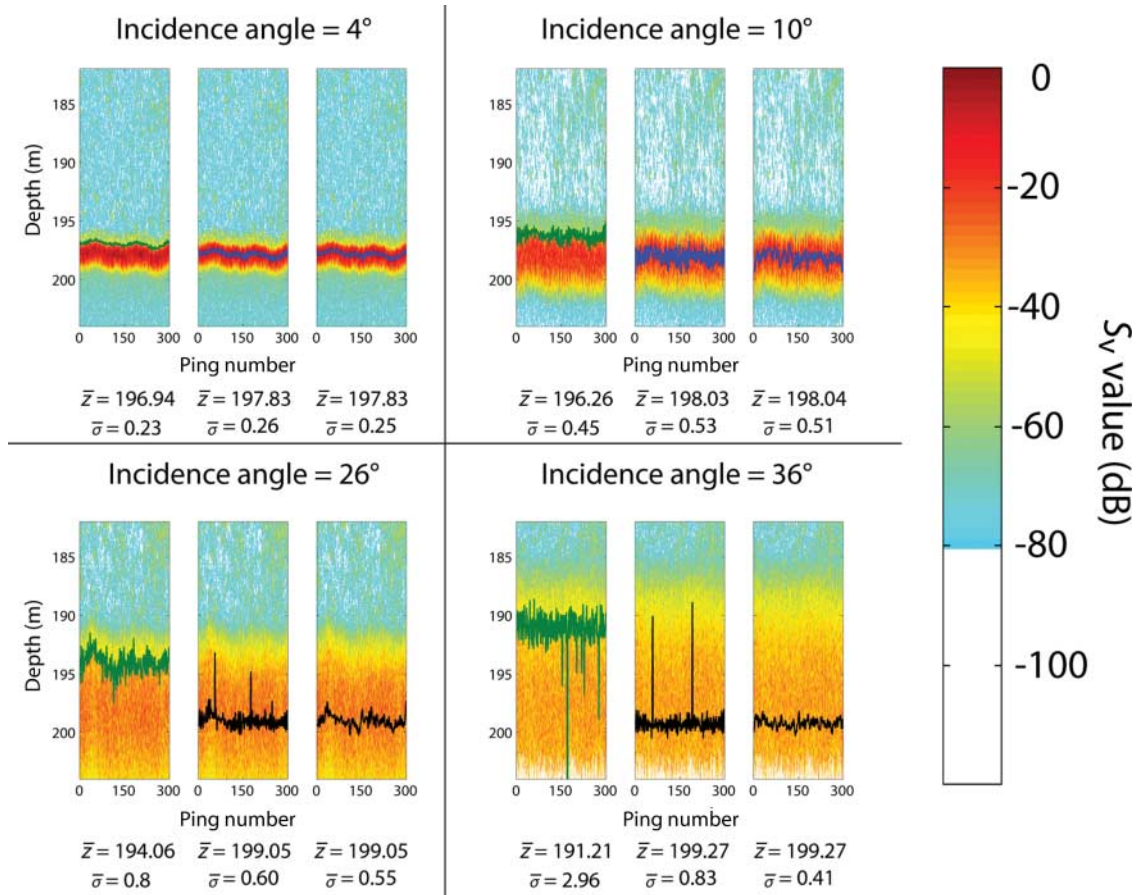
Figure 6. Four echograms of a scene at ~200-m depth, acquired by the ME70 during the EXACHA08 technological survey, for different incidence angles. For each angle, left: system bottom line, centre: bottom line after maximum-amplitude detection (blue) or phase-cancellation detection (black), right: bottom line after applying BCPF to the bottom line from the centre graph. In each case, numerical values are given for the mean estimated depth ($\bar{z}$) and the associated standard deviation ($\bar{\sigma}$).
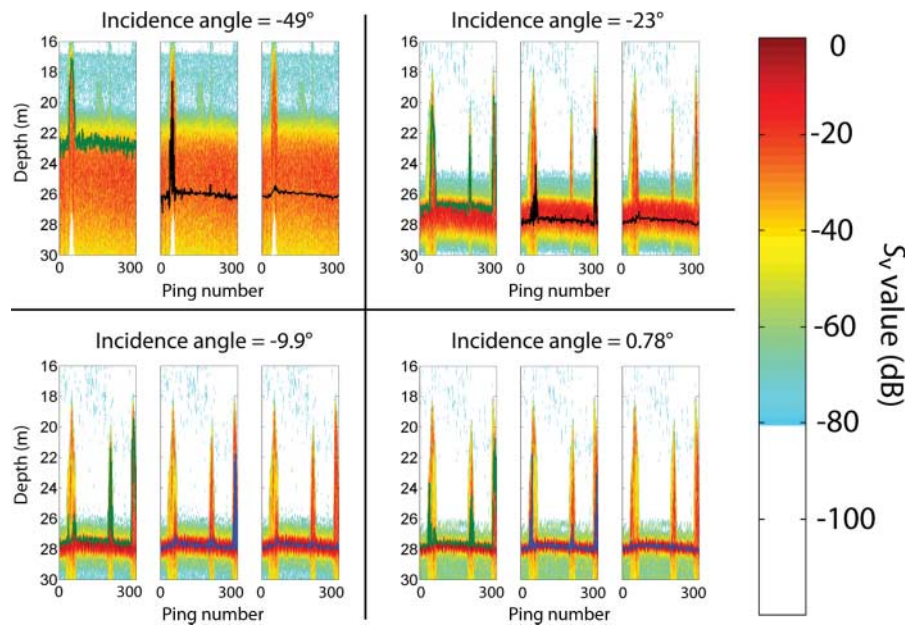

Figure 7. Four echograms of a scene at ~28-m depth, acquired by the ME70 during the IBTS08 survey, for different incidence angles. For each angle, left: system bottom line, centre: bottom line after maximum-amplitude detection (blue) or phase-cancellation detection (black), right: bottom line after BCPF was applied to the bottom line from the centre graph.

of the schools, amplitude-thresholding methods (left columns in Figure 7) were unable to detect the bottom below the fish schools, even in normal incidence.

Bottom-detection results without BCPF are illustrated in the centre columns of Figure 7. The incidence-angle limit for switching between maximum-amplitude and phase-cancellation methods was set to $\theta_{\lim} = 15°$. For smaller incidence angles, the maximum-amplitude method was more satisfactory than amplitude thresholding. It was noted, however, that the echo amplitude from fish was sometimes greater than that from the bottom. Thus, errors remained in the estimated bottom line. For higher incidences, the phase-difference signal was less sensitive to the presence of fish near the seabed. However, because the phase cancellation was searched in a region close to the amplitude-maximum, phase-based bottom detection was also liable to false detections. The BCPF algorithm was applied to each bottom-line detection independently, i.e. only the spatial continuity between two consecutive pings in the same beam was considered. Results are plotted in the right columns of Figure 7, proving that all spikes have been removed efficiently.

Conclusions

New methods were investigated to improve bottom detection with the ME70 echosounder. In each beam, bottom detection can be performed by locating the maximum of the echo amplitude for low incidence angles ($<15°$), or by detecting a cancellation in the athwartship phase-difference signal for incidence angles $>15°$. Applying the new methods to the processing of echograms acquired recently with the ME70 operating in split-beam mode yielded satisfactory results. However, such a detector still suffers from high variability and at times false bottom detections, especially at greater incidence angles and in deep water.

A state–space model for the seabed has been proposed, combined with an efficient particle-filter method, which efficiently stabilizes the detection; this is called the BCPF algorithm. Applications to both ER60 data in normal incidence and ME70 data for incidences between $-40°$ and $40°$ revealed that the BCPF also removes false detections caused by the presence of fish close to the seabed.

The approach presented here should be considered as a first attempt to improve bottom detection with the ME70 multibeam echosounder. Studies that are more extensive are needed to explore the limitations of the method and further development might improve on the robustness of the current version.

Satisfactory results were achieved with a reasonably flat or smoothly sloping seabed, but not for very irregular ground. In the latter case, the seabed-prediction model used for spatial regularity is poorly adapted to reality, while bottom prediction by the state–space model and raw echo-based detection can lead to contradictory information.

In the current version of the BCPF algorithm, no information about the bottom slope is extracted from the data. However, a slope estimate can be obtained from phase-difference data (Lurton, 2002). Such information could be usefully incorporated to improve the performance of the present algorithm.

References

Arulampalam, M. S., Maskell, S., Gordon, N., and Clapp, T. 2002. A tutorial on particle filters for online non-linear/non-Gaussian Bayesian tracking. IEEE Transactions on Signal Processing, 50: 174–188.

Carlson, T. J., and Jackson, D. R. 1980. Empirical evaluation of the feasibility of split-beam methods for direct *in situ* target-strength measurement of single fish. Applied Physics Laboratory Report, University of Washington, APL-UW 8006.

Doucet, A., de Freitas, N., and Gordon, N. 2001. Sequential Monte Carlo Methods in Practice. Springer, New York. 681 pp.

Edwards, A. W. F. 1972. Likelihood: an Account of the Statistical Concept of Likelihood and its Application to Scientific Inference. Cambridge University Press, Cambridge. 235 pp.

Ehrenberg, J. E. 1983. A review of *in situ* target-strength estimation techniques. FAO Fisheries Report, 300: 85–90.

Foote, K. G., Knudsen, H. P., Korneliussen, R. J., Nordbø, P. E., and Røang, K. 1991. Post-processing system for echo sounder data. Journal of the Acoustical Society of America, 90: 37–47.

Lurton, X. 2001. Précision de mesure des sonars bathymétriques en fonction du rapport signal/bruit. Traitement du signal, 18: 179–194.

Lurton, X. 2002. An Introduction to Underwater Acoustics: Principles and Applications. Springer, New York. 347 pp.

MacLennan, D. N., Copland, P. J., Armstrong, E., and Simmonds, E. J. 2004. Experiments on the discrimination of fish and seabed echoes. ICES Journal of Marine Science, 61: 201–210.

Misund, O. A. 1997. Underwater acoustics in marine fisheries and fisheries research. Reviews in Fish Biology and Fisheries, 7: 1–34.

Ona, E., and Mitson, R. B. 1996. Acoustic sampling and signal processing near the seabed: the deadzone revisited. ICES Journal of Marine Science, 53: 677–690.

Pouliquen, E., and Lurton, X. 1994. Identification de la nature du fond de la mer à l'aide de signaux d'échosondeurs: I. Modélisation d'échos réverbérés par le fond. Acta Acustica, 2: 113–126.

Simmonds, E. J., and MacLennan, D. N. 2005. Fisheries acoustics. *In* Theory and Practice, 2nd edn. Blackwell Publishing, Oxford. 437 pp.

Trenkel, V. M., Mazauric, V., and Berger, L. 2008. The new fisheries multibeam echosounder ME70: description and expected contribution to fisheries research. ICES Journal of Marine Science, 65: 645–655.

West, M., and Harrison, J. 1997. Bayesian forecasting and dynamic models. *In* Springer Series in Statistics, 2nd edn. Springer-Verlag, New York. 680 pp.